Materials Science in Semiconductor Processing 26 (2014) 199–204

Contents lists available at ScienceDirect

Materials Science in Semiconductor Processing

journal homepage: www.elsevier.com/locate/mssp

Electronic structure and magnetic properties of the perovskite cerium manganese oxide from ab initio calculations

Saadi Berri [a,b,*], Djamel Maouche [a], Miloud Ibrir [b], Badis Bakri [b]

[a] Laboratory for Developing New Materials and their Characterizations, University of Setif, Algeria
[b] Department of Physics, Faculty of sciences, University of M'sila, Algeria

ARTICLE INFO

Keywords:
Magnetic materials
Ab initio calculations
Spintronic

ABSTRACT

We have performed first-principle calculations of the structural, electronic and magnetic properties of cerium manganese oxide $(CeMnO)_3$, using full-potential linearized augmented plane-wave (FP-LAPW) scheme within GGA and GGA+U approaches. Features such as the lattice constant, bulk modulus and its pressure derivative are reported. Also, we have presented our results of the band structure and the density of states. The results show a half-metallic ferromagnetic ground state for $CeMnO_3$ in GGA+U treatment, whereas semi-metallic ferromagnetic character is observed in GGA. The results obtained, make the cubic $CeMnO_3$ a candidate material for future spintronic application.

1. Introduction

The cubic perovskites with varied compositions and structures have been extensively studied, motivated by their possible applications in numerous industrial and engineering domains [1–5]. They have showed a wide range of attractive properties ferroelectricity [6–8], piezoelectricity [9,10], semiconductivity [11], catalytic activity [12], thermoelectricity [13], superconductivity and metal-insulator transition [14]. As an example ternary oxides of rare earth (Eu, Gd, Tb)CoO_3 type oxides, this series reveal extensive applications in materials science and technology, some of the perovskites (Eu, Gd, Tb)CoO_3 compounds are used as electrode materials for magnetohydrodynamic (MHD) generators [15], for fuel cells [16]. On the other hand, perovskites like $BaMnO_3$ and $SrMnO_3$ have attracted interest in NO removal process as catalysts [17–19].

Lanthanoid-based peroviskite type oxides, such as $LaTMO_3$ (La: Lanthanoid, TM: transition metals), have been well-known as functional inorganic materials having a wide range of application for electrode materials of the alkaline fuel cell [20], ion sensor [21] and gas sensor[22–23]. The structural and electronic transport properties have been predicted for $La_{1-x}Ce_xMnO_3$ [24,25]. Generally, perovskites crystallize in orthorhombic structure, but many studies have depicted the cubic one [26–31].

Recently, half-metallic ferromagnetism has been found in CrO_2 [30], NiMnSb [31], Fe_3O_4 [32], $La_{0.67}Sr_{0.33}MnO_3$ [33], Co_2MnSi [34], Ti_2FeSi [35], Ti_2CoAl [36], NiCr(P, Se, Te, As) [37], Pb_2FeMoO_6[38], and CoFeMnZ (Z=Al, Ga, Si, Ge) [39], and nearly 100% high spin-polarization has been observed experimentally in the cases of CrO_2 and $La_{0.67}Sr_{0.33}MnO_3$ materials [40]. Half-metallic ferromagnets (HMF) meet all requirements of spintronics, as a result of their exceptional electronic structure. These materials behave like metals with respect to the electrons of one spin direction and like semiconductors with respect to the electrons of the other spin direction.

The considered $CeMnO_3$ is assumed to have ideal cubic perovskite structure (#221).

* Corresponding author at: Laboratory for Developing New Materials and their Characterizations, University of Setif, Algeria.
Tel.: +21395115576; fax: +213 36 92 72 10.
E-mail address: berrisaadi12@yahoo.fr (S. Berri).

http://dx.doi.org/10.1016/j.mssp.2014.04.027
1369-8001/

The cubic unit cell contains one molecule with the Wychoff positions of the atoms that are Ce 1a (0, 0, 0), Mn 1b (0.5, 0.5, 0.5) and O 3c (0.5, 0.5, 0). In the present paper, the structural, electronic and magnetic properties of $CeMnO_3$ compound are reported.

Our main goal in this work is to evaluate and examine the validity of the predictions of half metallicity for $CeMnO_3$ compound. The calculations are performed using ab initio full-potential linearized augmented plane wave (FP-LAPW) scheme within GGA and GGA+U approaches. Our paper is organized as follows. The theoretical background is presented in Section 2. Results and discussion are presented in Section 3. A summary of the results is shown in Section 4.

2. Method of calculations

We have carried out first-principle calculations [41,42] with both the full potential and linear augmented plane wave (FP-LAPW) method [43] as implemented in the WIEN2k code [44] within the density functional theory (DFT). The Perdew–Burke–Ernzerhof generalized gradient approximation GGA [45,46] and GGA+U [47]. In the calculations reported here, we use a parameter $R_{MT}K_{max}=9$, which determines matrix size (convergence), where K_{max} is the plane wave cut-off and R_{mt} is the smallest of all atomic sphere radii. We have chosen the muffin-tin radii (MT) for Ce, Mn and O to be 2.5, 1.8 and 1.6 a.u., respectively. Within the sespheres, the charge density and potential are expanded in terms of crystal harmonics up to angular momenta $L=10$, and a plane wave expansion has been used in the interstitial region. The value of $G_{max}=14$, where G_{max} is defined as the magnitude of largest vector in charge density fourier expansion. The Monkorst-Pack special k-points were performed using 3000 special k-points in the Brillouin zone. The cut off energy, which defines the separation of valence and core states, was chosen as -6 Ry. We select the charge convergence as 0.0001e during self-consistency cycles. The 4f orbital for the Ce atom was treated using the GGA+U approach with the values of $U=$ 7.07 eV, and $J=0.95$ eV(for Ce), and $U=4$ eV, $J=0.87$ eV for the 3d of the Mn [48].

3. Results and discussion

We have calculated the total energy as a function of lattice constant of $CeMnO_3$ compound for the ferromagnetic (FM) state. The plots of calculated total energies versus reduced volume of $CeMnO_3$ compound are shown in Fig. 1. The total energies versus changed volumes are fitted to the Murnaghan's equation of state [49] in order to determine the ground state properties, such as equilibrium lattice constant a, bulk modulus B and its pressure derivative B'. The calculated structural parameters of $CeMnO_3$ compound are reported in Table 1. Until now, an experimental or theoretical lattice constant, the bulk modulus and its pressure derivative value have not been reported. To the best of our knowledge, there are no experimental or theoretical data reported for the bulk modulus and its pressure derivative for the material of interest, and hence our results are predictions. We have also included in Table 1 the bulk modulus and its pressure derivative B' values for $PrMnO_3$ [50], $LaAlO_3$ [51], and $BaTiO_3$ [52] for comparison purpose. Note that the bulk modulus of $LaAlO_3$ and $BaTiO_3$ materials seems to be much larger than that of $CeMnO_3$ in both methods being considered here. This suggests that $CeMnO_3$ compound is less compressible than those materials.

The calculated spin-polarized band structures of $CeMnO_3$ compound at the theoretical equilibrium lattice

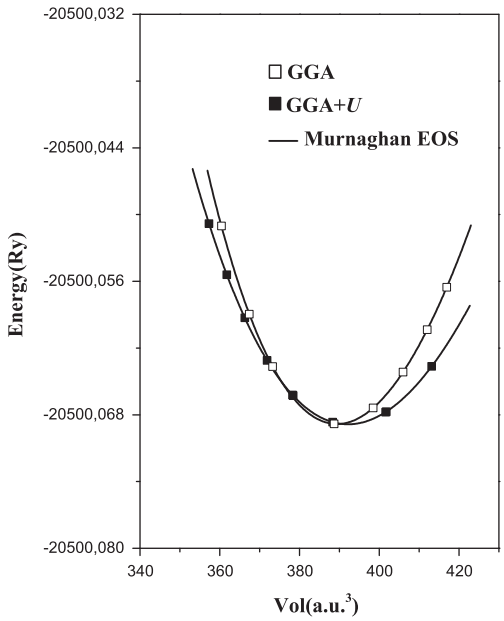

Fig. 1. Volume optimization for the $CeMnO_3$ compound.

Table 1
Lattice constant a(Å), bulk modulus B (in GPa), pressure derivative of bulk modulus B', total and partial magnetic moment (in μ_B) for $CeMnO_3$ compound.

Compound	a	B	B'	$m_{Ce,Pr}$	m_{Mn}	m_O	$m_{interstitial}$	m_{Total}
$CeMnO_3$								
GGA	3.87	141.95	3.83	0.898	3.054	0.053	0.898	4.353
GGA+U	3.91	147.88	3.62	0.988	3.818	−0.046	0.316	4.983
$PrMnO_3$ [50]								
GGA	3.88	–	3.5	2.18	3.23	0.04	0.41	5.94
GGA+U	3.85	–	4.23	2.29	3.35	−0.006	0.37	6
$LaAlO_3$ [51]								
GGA	3.81	193.17	4.29	–	–	–	–	–
$BaTiO_3$ [52]								
EXP	4	162	–	–	–	–	–	–

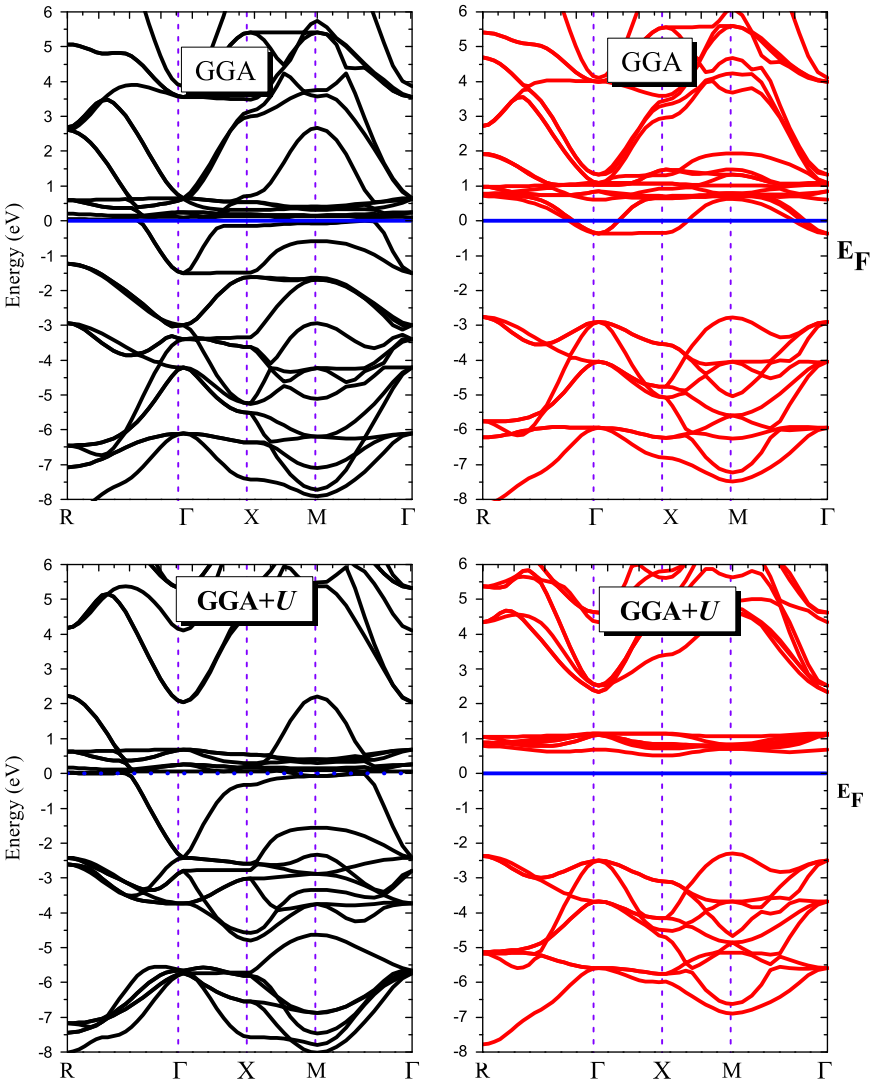

Fig. 2. The band structures of the $CeMnO_3$ compound for the spin-up and spin-down electrons.

constant along high-symmetry directions of the first Brillouin zone are shown in Fig. 2. The total and partial densities of states, in which the spin-up and spin-down sub-bands are plotted with black and red lines, respectively, are shown in Fig. 3. The Fermi level set as 0 eV.

In Fig. 2, we can see that for $CeMnO_3$ compound, the non-existence of a gap at Fermi level confirms the metallic behavior for GGA. On other hand, in the GGA+U method, it is clear that the majority-spin band is metallic, while the minority spin band shows a semiconducting gap around the Fermi level. In the minority-spin band, the valance band maximum (VBM) is located at −2.35 eV and the conduction band minimum (CBM) at 0.49 eV. The energy gap for spin-down electrons at around the Fermi level is 2.84 eV and close to the energy gap values for the $PrMnO_3$ compound [50]. This energy gap in the minority-spin band gap leads to 100% spin polarization at the Fermi level, resulting in the half-metallic behavior at equilibrium state.

In Fig. 3 shows the total density of states and partial density as a function of energy for the $CeMnO_3$ compound at its equilibrium lattice constant. To illustrate the nature of the electronic band structures, we have plotted the partial density of states (DOS) of Ce-f and d, Mn–d, and O–p electrons for the spin-up and spin-down sub-bands, the figure indicates that band structures can be divided into three parts: at the energy region from:(1) −8.0 to −3.0 eV we find the contribution of O–P electrons, (2) −3.0 to 2.0 eV, which reprsents the contribution of Ce–f hybridized with Mn–d orbital, (the exchange-splitting between the spin-up and spin-down sub-bands of the Mn–d and Ce–f states, which are the main contributors in the magnetic moment), and (3) 3.0 to 6.0 eV is from the contribution of Ce–d states.

The calculated total and atom-resolved magnetic moments, using GGA and GGA+U of $CeMnO_3$ compound, are shown in Table 1. The total magnetic moment which includes the contribution from the interstitial region arises from Ce and Mn ions with a small contribution of O atoms. The large exchange-splitting between the spin-up and spin-down sub-bands of the Mn–d and Ce–f states, which are the

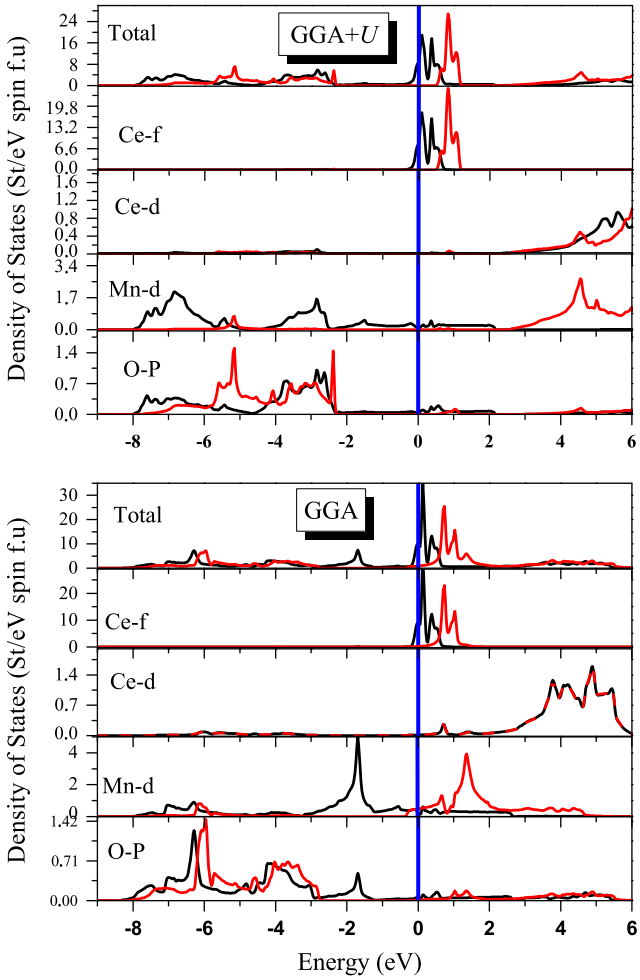

Fig. 3. Spin-polarized total densities of states (TDOS) and partial DOS.

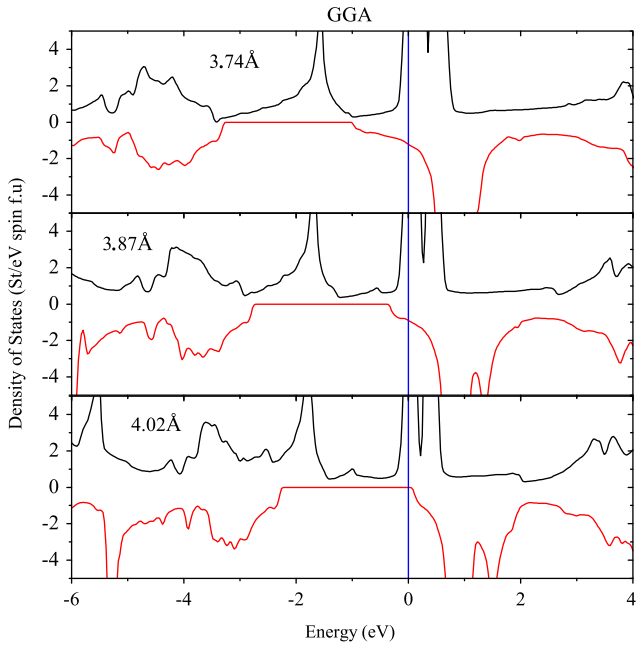

Fig. 4. Total TDOS for the $CeMnO_3$ compound as a function of the lattice constant using GGA.

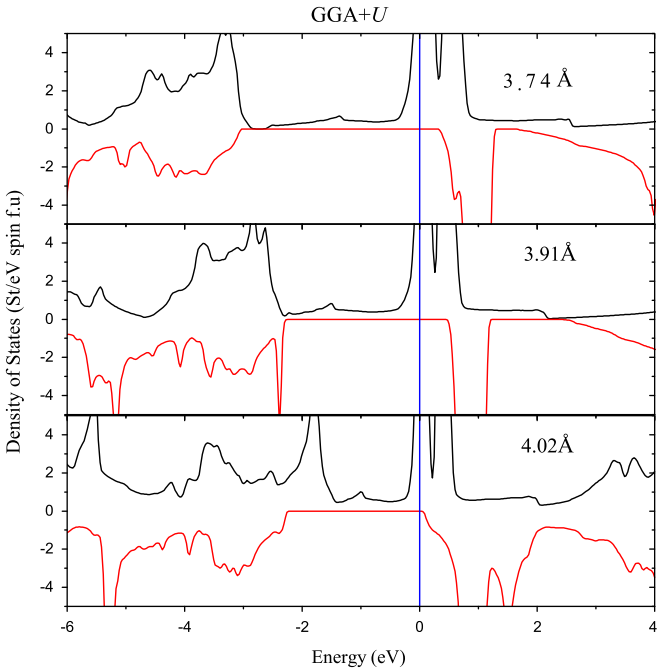

Fig. 5. Total TDOS for the $CeMnO_3$ compound as a function of the lattice constant using GGA+*U*.

main contributors in the magnetic moment. The present study shows that the total magnetic moment for $CeMnO_3$ compound is 4.353 μ_β for the GGA method. When we used the *U*-Hubbard term, the magnetic moment increased significantly. The magnetic moments of the Mn atoms (Table 1) are in agreement with theoretical data [50], the partial magnetic moments of the O atoms are very small.

In Figs. 4 and 5, the TDOS of $CeMnO_3$ compound at different lattice constants are presented for the GGA and the GGA+*U* method. In minority spin, with lattice expanding, a clear change of the Fermi level position is observed. All this retains a high spin polarization ratio of $CeMnO_3$ within the range studied 3.74–4.02 Å for the GGA+*U* method.

4. Conclusion

For the $CeMnO_3$ compound, the electronic structure and magnetic properties have been calculated using the first principles full-potential linearized augmented plane waves (FPLAPW) method. For $CeMnO_3$ compound, the magnetic moments are predominantly due to the Mn-3d and Ce-4d electrons. The electronic structure of the ferromagnetic configuration for $CeMnO_3$ compound has a metallic character. Although the local correlations treated via the GGA+*U* approach influence mainly the width of the energy gap. Therefore, the $CeMnO_3$ compound is a candidate material for future spintronic application.

References

[1] A. Soukiassian, W. Tian, V. Vaithyanathan, J.H. Haeni, L.Q. Chen, X. X. Xi, D.G. Schlom, D.A. Tenne, H.P. Sun, X.Q. Pan, K.J. Choi, C.B. Eom, Y.L. Li, Q.X. Jia, C. Constantin, R.M. Feenstra, M. Bernhagen, P. Reiche, R. Uecker, J. Mater. Res. 23 (2008) 1417–1432.
[2] H.W. Jang, S.H. Baek, D. Ortiz, C.M. Folkman, C.B. Eom, Y.H. Chu, P. Shafer, R. Ramesh, V. Vaithyanathan, D.G. Schlom., Appl. Phys. Lett. 92 (2008) 062910–062913.
[3] T. Wolfram, S. Ellialtioglu, Electronic and Optical Properties of d-Band Perovskites, Cambridge University Press, Cambridge, England, 2006, 280–303.
[4] A.K. Mikael, T.P. Comyn, A.J. Bell, Acta Mater. 56 (2008) 2110–2118.
[5] A.K. Azad, Synthesis, Structure, and Magnetic Properties of Double Perovskites of the type A_2MnBO_6 and A_2FeBO_6; (A=Ca, Sr, Ba, La; B=W), (Ph.D. Thesis), Gothenburg, University, Sweden, 2004.
[6] J.G. Bednorz, K.A. Muller, Phys. Rev. Lett. 52 (1984) 2289–2292.
[7] C.B. Samantaray, H. Sim, H. Hwang, Microelectron. J. 36 (2005) 725–728.
[8] C.B. Samantaray, H. Sim, H. Hwang, Physica B 351 (2004) 158–162.
[9] P. Baettig, C.F. Schelle, R Lesar, U.V. Waghmare, N.A. Spaldin, Chem. Mater. 17 (2005) 1376–1380.
[10] H. Wang, B. Wang, Q. Li, Z. Zhu, R. Wang, C.H. Woo, Phys. Rev B75 (2007) 245209–245217.
[11] H.P.R. Frederikse, W.R. Thurber, W.R. Hosler, Phys.Rev. 134 (1964) A442–A445.
[12] C.S. Koonce, M.L. Cohen, J.F. Schooley, W.R. Hosler, E.R. Pfeiffer, Phys. Rev 163 (1967) 380–390.
[13] V.E. Henrich, Rep. Prog. Phys. 48 (1985) 1481–1541.
[14] Xiao-Juan Liu, Zhi-Jian Wu, Xian-Feng Hao, Hong-Ping Xiang, Jian Meng, Chem. Phys. Lett. 11 (416) (2005) 7–13.
[15] D.B. Meadowcraft, P.G. Meier, A.C. Warren, Energy Convers. 12 (1972) 145–147.
[16] H.S. Spacil, C.S. Tedmon Jr., J. Electrochem. Soc. 116 (1969) 1618.
[17] H. Iwakuni, Y. Shinmyou, H. Yano, H. Matsumoto, T. Ishihara, Appl. Catal. 74 (2007) 299–306.
[18] H. Iwakuni, Y. Shinmyou, H. Yano, K. Goto, H. Matsumoto, T. Ishihara, Bull. Chem. Soc. Jpn. 81 (2008) 1175–1182.
[19] J. Zhu, A. Thomas, Appl. Catal., B, Environ 92 (2009) 225–233.
[20] D.B. Meadwcroft, Nature 226 (1970) 847–848.
[21] Y. Shimizu, A. Ishikawa, K. Iseki, S. Takase, J. Eletrochem. Soc. 47 (2000) 3931–3934.
[22] L. Zhang, H. Qin, P. Song, J. Hu, M. Jiang, Physics 98 (2006) 358–362.
[23] Y.L. Chai, D.T. Ray, G.J. Chen, Y.H. Chang, J. Alloys Compo. 333 (2002) 147–153.
[24] S. Husain, R.J. Choudhary, R. Kumar, S. Patil, J.P. Srivastava, Indian Acad. Sci. 58 (2002) 1045–1049.
[25] W.J. Kuen, L.K. Pah, A.H. Shaari, Ch.S. Kien, N.S. Wei, A.G.H. Ming, J, Technol 20 (2012) 73–78.

[26] Y.P Yadava, E. Montarroyos, J.M Ferreira, J.A. Aguiar, Phys, C: Superconduct. 354 (2001) 444–448.
[27] J.M. Porras-Vazquez, P.R. Slater, J. Power Sour. 209 (2012) 180–183.
[28] D.A. Landínez Téllez, D. Llamosa, P.C.E. Deluque Toro, A.V.G. Rebaza, J.R. Rojas, J. Mol. Struct. 1034 (2013) 233–237.
[29] A. Zahid, A. Iftikhar, I. Khan, B. Amin., Intermetallics 31 (2012) 287–291.
[30] S.M. Watts, S. Wirth, S. von Molnar, A. Barry, J.M.D. Coey, Phys. Rev. B 61 (2000) 9621–9628.
[31] R.A. de Groot, F.M. Mueller, P.G. van Engen, K.H.J. Buschow, Phys. Rev. Lett. 50 (1983) 2024–2027.
[32] A. Yanase, H. Siarori, J. Phys. Soc. Jpn. 53 (312) (1984);
F.J. Jedema, A.T. Filip, B. van Wees, Nature 410 (2001) 345–348.
[33] W.E. Pickett, D.J. Singh, Phys. Rev. B 53 (1996) 1146–1160.
[34] M.P. Raphael, B. Ravel, M.A. Willard, S.F. Cheng, B.N. Das, R.M. Stroud, K.M. Bussmann, J.H. Claassen, V.G. Harris, Appl. Phys. Lett. 79 (2001) 4396–4398.
[35] Nazmiye Kervan, Selcuk Kervan, J. Phys. Chem. Solids 72 (2011) 1358–1361.
[36] Eser Bayar, Nazmiye Kervan, Selcuk Kervan, J. Magn. Magn. Mater. 323 (2011) 2945–2948.
[37] E. Sasiog-brevelu, L.M. Sandratskii, Bruno, J. Appl. Phys. 98 (2005). (063523-063523-6).
[38] Yan Zhang, Vincent Ji, J. Phys. Chemi. Solids 73 (2012) 1116–1121.
[39] V. Alijani, S. Ouardi, G.H. Fecher, J. Winterlik, S.S. Naghavi, X. Kozina, G. tryganyuk, C. Felser, E. Ikenaga, Y. Yamashita, S. Ueda, K. Kobayashi, Phys. Rev. B 84 (2011) 224416–224425.
[40] G.M. Muller, J. Walowski, M. Djordjevic, G.-X. Miao, A. Gupta, A. V. Ramos, K. Gehrke, V. Moshnyaga, K. Samwer, J. Schmalhorst, A. Thomas, A. Hutten, G. Reiss, J.S. Moodera, M. Munzenberg, Nat. Mater. 8 (2009) 56–61.
[41] P. Hohenberg, W. Kohn, Phys. Rev. B 136 (1964) 864–871.
[42] W. Kohn, L.J. Sham, Phys. Rev. A 140 (1965) 1133–1138.
[43] J.C. Slater, Adv. Quant. Chem 1 (1964) 5564–5591.
[44] P. Blaha, K. Schwarz, G. K. H. Madsen, D. Kvasnicka, J. Luitz, WIEN2K, an Augmented Plane Wave +Local orbitals program for calculating crystal properties Karlheinz Schwarz, Technische Universität, Wien, Austria, 2001, ISBN 3-9501031-1-2.
[45] J.P. Perdew, K. Burke, Y. Wang, Phys. Rev. B 54 (1996) 16533–16539.
[46] J.P. Perdew, S. Burke, M. Ernzerhof, Phys. Rev. Lett 77 (1996) 3865–3868.
[47] C. Loschen, J. Carrasco, K.M. Neyman, F. Illas, Phys. Rev. B 75 (2007) 35115–1–035115–8.
[48] M. Chakraborty, P. Pal, B.R. Sekhar, Solid State Commun. 145 (2008) 197–200.
[49] F.D. Murnaghan, Proc. Nat. Acad. Sci. USA 30 (1944) 244–247.
[50] B. Bouadjemi, S. Bentata, A. Abbad, W. Benstaali, B. Bouhafs, Solids Stat. Commun. 168 (2013) 6–10.
[51] A. Boudali, B. Amrani, M. Driss khodja, A. Abada, K. Amara, Comput. Mater. Sci. 45 (2009) 1068–1072.
[52] K.H. Hellwge, A.M. Hellwege, Ferroelectrics and Related Substances, New Series, Vol. 3, Landolt-Bornstein, Springer Verlag, Berlin, 1969.